Available online at www.sciencedirect.com
SCIENCE DIRECT
Journal of Catalysis 232 (2005) 226–238
JOURNAL OF CATALYSIS
www.elsevier.com/locate/jcat

Bridging the pressure and material gap in the catalytic ammonia oxidation: structural and catalytic properties of different platinum catalysts

M. Baerns [a,*], R. Imbihl [b,*], V.A. Kondratenko [a], R. Kraehnert [a], W.K. Offermans [c], R.A. van Santen [c,*] A. Scheibe [b],

[a] *Institute for Applied Chemistry Berlin-Adlershof, Richard-Willstätter-Str. 12, D-12489 Berlin, Germany*
[b] *Institut für Physikalische Chemie und Elektrochemie, Universität Hannover, Callinstr. 3-3a, 30167 Hannover, Germany*
[c] *Schuit Institute of Catalysis, Eindhoven University of Technology, PO Box 513, 5600 MB Eindhoven, The Netherlands*

Received 14 September 2004; revised 22 February 2005; accepted 1 March 2005

Available online 12 April 2005

Abstract

To understand the "pressure and material gap" in the platinum-catalyzed ammonia oxidation over Pt, the reaction was studied over a wide range of pressures (10^{-3}–10^{5} Pa) and temperatures (293–1073 K) with different Pt catalysts: stepped Pt(533) single crystal, knitted Pt gauze, and Pt foil. Experiments were supplemented by theory applying DFT calculations. It was concluded that the primary reaction step of NH_3 oxidation, stripping of hydrogen from the NH_3 molecule, is favored by the presence of surface O and OH species. The latter species are more active for dehydrogenation of NH_2 and NH fragments. NO and N_2 are the only nitrogen-containing products detected under UHV conditions ($p < 10^{-1}$ Pa). N_2O was observed, however, at about 6 Pa (peak pressure) in the temporal analysis of products (TAP) reactor and under ambient pressure conditions of 100 kPa in a microstructured reactor. The pressure dependence of N_2O formation is suggested to be related to a minimum surface coverage by reaction intermediates required for N_2O formation, which is a real "pressure gap" phenomenon. Independently of the pressure range (10^{-3}–10^{5} Pa) and the type of Pt specimen, N_2 formation prevails at low temperatures (< 700 K), whereas NO production increases with temperature and becomes the dominant reaction channel at high temperature. Catalyst characterization by SEM revealed a reconstruction of the Pt surface after ammonia oxidation at ambient pressure. The degree of surface restructuring is related to the total exposure of the catalyst to the reactants. Surface roughening contributes to activation of the catalyst and changes in its selectivity.

Keywords: Ammonia oxidation; Platinum; NH_3; N_2O; Microstructured reactor; TAP reactor; UHV reactor; SEM; Surface restructuring of Pt catalysts

1. Introduction

Selective oxidation of ammonia to nitric oxide over platinum-group metal (PGM) catalysts is the essential reaction of industrial manufacture of nitric acid, which is one of the most important bulk chemicals. The oxidation of ammonia comprises mainly the exothermic oxidation of NH_3 to NO; however, in addition, other side reactions with significant exothermicity occur, affecting the overall reaction. It is commonly accepted that the process is mass-transfer limited at ambient and elevated pressures [1–6]. The reaction has been studied for a very broad range of temperatures (300–1500 K), pressures (10^{-8}–10^{5} Pa), and over different materials (Pt single crystal [7–11], polycrystalline Pt [12–18], supported Pt [19]). Despite the fact that oxidation of ammonia over PGM gauzes is a highly optimized and balanced industrial process, there is neither a generally accepted mechanism nor intrinsic kinetics of all the reaction steps involved in the catalytic ammonia oxidation. Difficul-

* Corresponding authors.
E-mail addresses: baerns@aca-berlin.de (M. Baerns), ronald.imbihl@mbox.pci.uni-hannover.de (R. Imbihl), r.a.v.santen@tue.nl (R.A. van Santen).

0021-9517/$ – see front matter
doi:10.1016/j.jcat.2005.03.002

ties in the study of intrinsic kinetics of ammonia oxidation are caused by a lack of temperature control of the exothermic reaction (ignition, temperature gradients) and mass-transfer limitations. Therefore, most mechanistic studies of ammonia oxidation were performed under ultrahigh-vacuum (UHV) conditions [12,13,20–22], under which isothermicity is achieved. The oxidation of ammonia reveals a strong temperature dependence of product selectivity. N_2 is the main product at low temperatures (< 600 K); NO production dominates above 800 K [13,20,22]. However, N_2 production prevails again when the temperature is increased further to 1473 K. In mechanistic and kinetic studies of ammonia oxidation at UHV pressures, no information about nitrous oxide formation is obtained, since this product was never observed under such conditions, in contrast to continuous-flow studies at ambient pressure [14,18]. In industrial ammonia converters, operating above 1073 K, the concentration of N_2O in the tail gas can reach 3000 ppmv [23], which is a severe environmental issue.

To overcome ignition limitations, the kinetics of ammonia oxidation was recently studied at low temperature (up to 650 K) over alumina supported Pt in a combined microstructured reactor and heat exchanger device at a total pressure of 1 bar and in a large excess of oxygen [14,24,25]. Because of improved heat transfer in this reactor, the ignition of NH_3–O_2 mixtures could be avoided up to 650 K [25]. N_2O was observed as a reaction product. However, the authors did not focus on catalyst characterization before and after the catalytic reaction, which is an important aspect of the ammonia oxidation reaction that is known to induce major changes in catalyst morphology. Moreover, no explanation of the differences in product distribution under UHV and ambient-pressure conditions was given. More recently, the temporal analysis of products (TAP) reactor was shown to be an excellent tool for studying ammonia oxidation over industrially relevant Pt and Pt–Rh gauzes under isothermal conditions at temperatures of industrial ammonia burners (1023–1073 K) [26]. N_2O was identified as a reaction product [27]. The peak pressure in the TAP reactor was ca. 160 Pa at 1073 K.

Operation of the catalysts under industrial conditions is accompanied by strong restructuring of the surface, resulting in development of “cauliflower” structures. These changes occur during the first hours of operation and are assumed to play an important role in improving catalytic performance [28]. The phenomenon was the subject of a number of high-temperature (> 900 K) studies [15–17,29,30]. The development of facets depends strongly on the partial pressure of O_2 and NH_3 and surface temperature, resulting in different surface structures (flat and curved surfaces, pits) [16]. SEM studies of Lyubovsky and Barelko [15] have shown that restructuring occurs in two stages, with initial formation of parallel facets followed by growth of micro crystals. The initial facet formation is not uniform on all grains; this is probably due to the structure sensitivity of reaction and faceting [15]. No restructuring was observed during ammonia oxidation up to a total pressure of 15 Pa, even over a long period of catalyst operation [13,20].

It is obvious from the above background that for a detailed understanding of ammonia oxidation, the reaction should be studied under well-defined surface properties of the catalyst and isothermal reaction conditions, emphasizing the identification of all possible reaction products and short-lived reaction intermediates. For these purposes, a microstructured reactor made of quartz glass, the TAP reactor, and an UHV reactor were applied. The experimental results of this study are discussed for a broad range of total pressures (10^{-3}–10^5 Pa), temperatures (293–1073 K), and materials: stepped Pt single-crystal (Pt(533)), polycrystalline Pt foil, and industrial knitted Pt gauze. Particular attention was paid to reaction-induced catalyst restructuring. In addition, density functional theory (DFT) calculations were performed to study the role of oxygen-containing surface species in the oxidation of NH_3.

2. Experimental

First the catalytic Pt materials used in this study are described (Section 2.1). Since the ammonia oxidation was studied over a wide range of pressures (10^{-3}–10^5 Pa), suitable reactors were required for the various pressures, which are presented in Section 2.2. Finally, details of the experimental procedure, DFT calculations, and catalyst characterization are given in Sections 2.3–2.5.

2.1. Catalytic material

Three different Pt materials were used in this study. Ambient-pressure catalytic tests were carried out with platinum foil (99.95%) supplied by Alfa Aesar. The foil thickness was 4 μm. TAP experiments were performed over knitted Pt gauze (Multinit type 4; Degussa) with a wire diameter of 76 μm. A Pt(533) single crystal was used for UHV studies. The Pt(533) surface, Pt 4(111) × (100), consists of four-atom-wide (111) terraces followed by monoatomic (100) steps.

2.2. Experimental setup

2.2.1. Microstructured reactor

Temperature control is an essential issue in fundamental studies of the catalytic ammonia oxidation. Neither mechanistic insights nor kinetic data could be obtained in a plug flow reactor at ambient pressure over Pt gauze because of the high exothermicity of the reaction and the related temperature runaway. However, these obstacles were overcome with a microstructured flow reactor, which ascertained:

– Good mass transfer due to short diffusion paths in the microstructures (hydrodynamic diameter of reactor channel $d_h = 375$ μm);

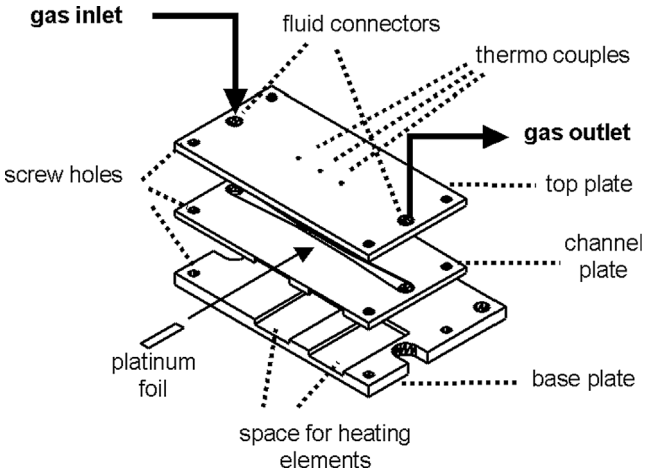

Fig. 1. Exploded view of micro-structured quartz reactor with Pt foil catalyst.

– Good temperature control along the catalyst; this was due to the large ratio between the heat exchange area and the active surface area (1:1), which were both equal to the area of the reactor wall;
– The low blank activity of the reactor walls made of SiO_2;
– The ability to quickly reach high temperatures (no sealing was located in the hot reaction zone; a temperature of 850 K was reached within 2 min).

In contrast to previous studies of ammonia oxidation in a microstructured reactor made of stainless steel [14,24,25], which were performed over a supported Pt catalyst up to 650 K, the present microstructured reactor, made from silica, allowed us to study ammonia oxidation over bulk Pt catalysts up to 850 K under isothermal conditions. An exploded view of the microstructured reactor is shown in Fig. 1. The reactor consisted of three plates made of quartz glass stacked on top of each other. The total length of the reactor was 125 mm. The plates had been microstructured by sand blasting. The middle plate carried two reaction channels, each 500 μm wide and 300 μm deep. They were connected to the gas inlet and outlet by broader channels. Two holes ("gas inlet," "gas outlet") at the end of the gas channels permitted fixing of the fluid connectors. Holes at the corners of the plate were used to connect the plates with screws. Additional clamps assured gas-tight sealing up to 1.3×10^5 Pa. The upper side of the top plate contained conical holes for thermocouples at specified locations. Material had been removed from the quartz-glass walls (by sandblasting) to provide space for two ceramic heating elements. We mounted a strip of the Pt foil catalyst (10 mm deep, 4 μm thick, < 2 mm wide) on top of the channels by fixing it between the top and channel plates. Only two 500-μm-wide areas of Pt foil were exposed to the gas flow. Thus, the thin Pt catalyst was located on the upper wall of the microstructured channels and had good contact with the channel wall.

A ceramic heating element was placed in the center of symmetry (with respect to the flow direction) of the reactor, the reaction zone, and was used to control the catalyst temperature. According to CFD simulations and temperature measurements in the gas channel, a temperature profile develops along the channel axis during operation with a flat and broad maximum in the zone of the (15-mm-wide) central heating element. The catalyst (< 2 mm wide) was mounted in the center of the broad maximum, providing a measured axial temperature deviation less than 5 K in the catalyst range. The heat released by the exothermic ammonia oxidation was small ($< 1\%$) compared with the supplied electrical power that was required to keep the desired temperature level. Thus, the assumption of isothermicity holds.

2.2.2. Temporal analysis of products reactor

The temporal analysis of products (TAP-2) reactor applies a pulse technique under vacuum conditions [31,32]. The unique features of the TAP reactor for mechanistic studies of high-temperature ammonia oxidation under isothermal conditions were previously reported [26]. Depending on the pulse size (10^{13}–10^{17} molecules), the gas transport in the catalytic reactor is determined by either Knudsen or molecular diffusion. In the present study all experiments were performed in the Knudsen diffusion regime ($< 10^{15}$ molecules/pulse). Since under such conditions collisions between molecules in the gas phase are negligible, solely heterogeneous interactions were observed. This also opens up the possibility for detecting short-lived reaction intermediates, when they escape in the gas phase, and if their concentration is not below the detection limit of QMS (quadrupole mass spectrometry) analysis. Transient experiments up to 1073 K were carried out in a homemade quartz-glass reactor.

2.2.3. UHV reactor

A standard UHV system equipped with LEED, a retarding field analyzer for Auger electron spectroscopy, a scanning tunneling microscope, and a differentially pumped quadrupole mass spectrometer (QMS) was used for rate measurements. Under reaction conditions the UHV system was operated as a continuous-flow reactor. During rate measurements the cone (opening 2 mm), which connected the differentially pumped QMS with the main vacuum chamber, was brought 1 mm in front of the surface. In this way reaction products from the back of the sample and from filaments were excluded.

2.3. Experimental procedure

2.3.1. Flow studies in the microstructured reactor close to ambient pressure

Catalytic tests were carried out with feeds of different compositions and a Pt foil "as received." Concentrations of NH_3 (99.8%) and O_2 (99.98%) were up to 3 and 4.5 vol%,

respectively. The concentration of Ne (99.99%) as an internal standard was always 10 vol%; the balance was Ar (99.99%). All gases were dosed by electronic mass flow controllers. For temperature-programmed ammonia oxidation, a flow of fixed composition was fed to the reactor at room temperature, then the temperature in the catalyst zone of the reactor was changed stepwise (25, 50, and 100 K). Temperature was held constant at each level for at least 20 min. Blank activity in the whole temperature range (300–833 K) was found to be too low to be measured. Effluent gas composition was continuously monitored by QMS (Balzer Omnistar GSD 300). For quantitative evaluation, all of the feed components and reaction products were calibrated with respect to Ne. Back pressure was adjusted by a needle valve to 102 kPa. Feed gas composition was measured in each experiment during blank runs at room temperature.

We tested mass transfer limitation of the fast reaction by replacing the diluting gas Ar with He in the catalytic experiments at various temperatures. Diffusion coefficients in He are significantly higher (approximately twofold) than in Ar and, hence, result in higher mass transfer coefficients. Thus, deviations between the measurements with Ar and He indicate that mass transfer influences catalytic results [33].

2.3.2. Pulse studies in the TAP reactor under vacuum conditions

The Pt gauze (0.119 g) was packed (packing density 4.2×10^3 kg m^{-3}) between two layers of quartz particles ($d_p = 250$–355 μm) in the isothermal zone of the quartz TAP microreactor (i.d. = 0.006 m, $L = 0.04$ m). Before the experiments the Pt gauze was pretreated at ambient pressure in a flow of 30 ml min^{-1} of pure oxygen at 1073 K for 1 h to remove carbon deposits. Before pulse experiments with NH_3 the gauze was additionally pretreated with O_2 pulses before each experiment to recover the loss of oxygen species in the previous experiment. Interaction of ammonia with oxygen-free Pt was performed after pretreatment in a flow of 10 ml min^{-1} of pure H_2 at 1073 K for 4 h. After any pretreatment the Pt gauze was exposed to vacuum conditions (10^{-6} Pa). Then, pulses containing a small amount of reactant ($< 5 \times 10^{14}$ molecules per pulse, resulting in a peak pressure of ca. 6 Pa) were injected into the microreactor.

Transient experiments were carried out in the temperature range between 323 and 1073 K with steps of 100 K, with mixtures of $O_2/{}^{14}NH_3/Ne = 1{:}1{:}1$, $O_2/{}^{15}NH_3/Ne = 1{:}1{:}1$, $O_2/{}^{14}NH_3/Ne = 2{:}1{:}1$, or $NH_3/Ne = 1{:}1$. Transient responses of reactants and products were analyzed at the reactor outlet by mass spectroscopy at atomic mass units (AMUs) related to N_2O (44.0, 30.0, 28.0), O_2 (32.0), NO (30.0), N_2 (28.0), H_2O (18.0), NH_3 (15.0), Ne (20.0), and Xe (132.0). In experiments with a mixture of ${}^{15}NH_3/O_2/Ne = 1{:}1{:}1$, transient responses were recorded at AMUs ${}^{15}N_2O$ (46.0, 31.0, 30.0), O_2 (32.0), ${}^{15}NO$ (31.0), ${}^{15}N_2$ (30.0), and Ne (20.0). When a signal was not unique for one component, this is indicated in the text and the figures. In all experiments, pulses were repeated 10 times for each AMU and averaged to improve the signal-to-noise ratio. Ne (99.998%), Xe (99.99%), O_2 (99.995%), ${}^{14}NH_3$ (99.98%), and ${}^{15}NH_3$ (99.9%) were used without further purification. Isotopically labeled ammonia was purchased from ISOTEC (USA).

Blank tests with NH_3–O_2 mixtures in the TAP reactor filled with SiO_2 particles showed only very low activity at temperatures higher than 1023 K. The main product of the blank runs was nitrogen; its molar fraction was lower than 0.01 even at 1073 K.

2.3.3. Flow studies in the UHV reactor

Samples were prepared by repeated cycles of Ar^+ bombarding ($E = 1$ keV, $p_{Ar} = 2 \times 10^{-3}$ Pa, $t = 15$ min), heating in oxygen ($p_{O_2} = 1 \times 10^{-4}$ Pa), followed by annealing to 1300 K. The heating and cooling rate in the temperature cycling experiments was 100 K min^{-1}. Gases of purity 99.99% for oxygen and 99.5% for ammonia were used. All pressures given for the UHV studies are uncorrected. NO formation was followed in a QMS via an AMU of 30 and N_2 via an AMU of 28. The CO contribution to the signal of AMU 28 was determined from the signal of an AMU of 12 originating from CO fragmentation and then subtracted. The background was taken from rate measurements at 300 K, with the assumption that the catalytic activity at this temperature is negligible. To determine the absolute reaction rates, the QMS was calibrated against the ionization gauge in the main chamber.

2.4. DFT calculations

Electronic structure calculations within the framework of density functional theory (DFT) were performed with the VASP code [34,35]. Ultrasoft pseudo-potentials, introduced by Vanderbilt [36] and generated by Kresse and Hafner [37], were used to describe the ion-electron interactions. The one-electron Kohn–Sham eigenfunctions were expanded in plane waves with an energy cutoff of 400 eV. The PW-91 functional accounting for the exchange-correlation of the electrons was included in the code and exploited for the calculations [38]. A platinum slab, formed by a periodical expansion of a unit cell (supercell approach), consisting of five layers of Pt atoms and separated by five metal layers replaced by vacuum (∼ 13.8 Å), served as an adsorbent. Adsorbates were adsorbed on both sides of the slab, maintaining S_2 space group symmetry. In such way we prevented long-range dipole–dipole interactions between mirror unit cells. We used a DFT-optimized Pt–Pt bond length of 2.82 Å instead of the experimental bulk distance of 2.77 Å to avoid unrealistic forces on the metal atoms. A uniform 5×5 k-point sampling mesh within the first Brillouin zone, obtained via the Monckhorst package, was applied. The k-point summation was done with an electronic temperature of 0.15 eV, and the total energy was extrapolated to zero temperature. Since in previous work on the O/Pt(111) and NO/Pt(111) adsorbate system [39] and comparable adsorbate systems like O/Ru(0001) [40] and O/Pd(211) and NO/Pd(211) [41]

no net magnetization was found, we assumed that the magnetic moment of the adsorbates was totally quenched by adsorption to the slab. Therefore, all of our calculations were done in a non-spin-polarized way, except for open shell atoms and molecules in the "gas phase." The minimum energy path (MEP) for the reactions was determined by the nudged elastic band method (NEB) [42,43] with improved tangent estimate [44]. The goal of the NEB search was to find a configuration close to the transition state (TS) of the reaction. This configuration was further optimized with a quasi-Newton algorithm to minimize the forces and hence to determine the equilibrium position of the TS. In some subtle cases, it turned out to be necessary to refine this TS search with "smarter" NEB methods, like the climbing image nudged elastic band (CI-NEB) and variable nudged elastic band (VNEB) methods [45].

In all the calculations the total energy converged to approximately 5 kJ mol^{-1} with respect to the *k*-point sampling, energy cutoff, and cell size. If not otherwise stated, no restrictions on the atoms were implied for geometry optimization.

2.5. Catalyst characterization

To follow surface-morphology changes of the catalysts, they were characterized by scanning electron microscopy (SEM) before and after exposure of the catalyst to ammonia oxidation. Images were recorded on a Hitachi-S4000 equipped with a field emission gun (FEG) (cold) in SE mode. The electron accelerating voltage was 15 kV.

3. Results

First, results from theoretical and experimental studies on the role of oxygen-containing surface species in NH_3 decomposition/activation are presented. Then, data for catalytic ammonia oxidation on polycrystalline Pt foil, knitted Pt gauze, and a single Pt(533) crystal under ambient pressure, low vacuum (ca. 6 Pa), and UHV conditions, respectively, are shown. The catalytic data are supplemented by SEM images of the respective catalyst surfaces. Thereafter, the information will be compared and discussed, with the intention of understanding those factors that influence surface restructuring and product distribution as a function of total pressure.

3.1. Ammonia activation on Pt surfaces

In a broad temperature range (323–1073 K), no gas-phase reaction products were observed with NH_3 pulsing over Pt gauze pretreated with hydrogen. Hence, a hydrogen-treated Pt surface is inactive for NH_3 decomposition at short residence times (10^{-3} s) in the TAP reactor. In contrast, Pt gauze pretreated with O_2 shows high activity for NH_3 conversion (see Fig. 2). As shown previously [49], ammonia adsorbs

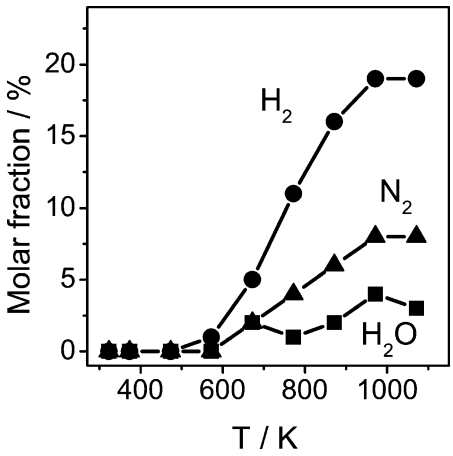

Fig. 2. Molar fractions of N_2, H_2O and H_2 vs. temperature when $^{14}NH_3/Ne = 1/1$ mixture was pulsed in the TAP reactor over Pt gauze having been pre-treated in O_2.

on oxygen-covered single-crystal surfaces of Pt(443) and Pt(533) with a high reactive sticking coefficient up to 0.2. Since ammonia decomposition on the bare Pt surfaces is negligible below 600 K, adsorbed oxygen clearly activates ammonia decomposition on Pt. Therefore it can be concluded from experimental results that stripping of hydrogen atoms from the NH_3 molecule by oxygen species is the dominating primary reaction step in the activation of ammonia. This conclusion is consistent with results obtained in UHV studies on Pt(111) [21] and Pt(100) [8], as well as for studies on Pt sponge up to 573 K [46]. As outlined below, this is also in agreement with theoretical considerations. N_2, H_2, and H_2O were the only reaction products observed at the reactor outlet with NH_3 pulsing over O_2-treated Pt gauze (Fig. 2). Nitric oxide and nitrous oxide were not observed. N_2 formation started above 573 K and increased continuously with temperature, in contrast to the temperature dependence of N_2 formation found in experiments with different NH_3–O_2 mixtures, as described in Section 3.3 (Figs. 5 and 6). H_2 and H_2O were detected as hydrogen-containing products in experiments on NH_3 pulsing in the absence of gas-phase O_2 (Fig. 2), where hydrogen was the main product. However, H_2O was the only hydrogen-containing product observed when NH_3–O_2 mixtures were pulsed over Pt gauze (Figs. 5 and 6). For discussion of these differences see Section 4.2.

To further evaluate the reaction pathways of ammonia activation by adsorbed oxygen-containing species, NH_3 decomposition over a flat Pt(111) surface was studied by DTF calculations. The (111) surface is usually assumed to be the main face of polycrystalline Pt. In Table 1 the energy profiles are presented for the reaction of ammonia on a Pt(111) surface without co-adsorbed species, in the presence of adsorbed oxygen atoms, and in the presence of hydroxyl groups. We performed the respective calculations while considering computed binding energies and adsorption-site preferences of possible intermediates, reactants, and products of ammonia oxidation evaluated by Offermans et al. [47]. The activation energy for the abstrac-

Table 1
Reaction barrier E_{act}[a] and energy change ΔE[a] for the dehydrogenation of NH_x on Pt{111}

Reaction	E_{act} (kJ mol^{-1})	ΔE (kJ mol^{-1})
$NH_3 \rightarrow NH_2 + H$	112	51
$NH_2 \rightarrow NH + H$	131	−4
$NH \rightarrow N + H$	134	39
$NH_3 + O \rightarrow NH_2 + OH$	41	41
$NH_2 + O \rightarrow NH + OH$	122	−14
$NH + O \rightarrow N + OH$	145	29
$NH_3 + OH \rightarrow NH_2 + H_2O$	30	−15
$NH_2 + OH \rightarrow NH + H_2O$	0	−67
$NH + OH \rightarrow N + H_2O$	43	−25

[a] E_{act} and ΔE are determined from the energy difference between the most stable initial and the lowest transition state and between the initial and final states respectively, neglecting possible lateral interactions.

tion of hydrogen atoms from NH_3 molecules is lowered by both chemisorbed oxygen and hydroxyl species. Most importantly, adsorbed oxygen atoms only decrease the activation barrier for the abstraction of the first hydrogen atom from NH_3 molecules significantly, whereas OH species allow easier abstraction of all hydrogen atoms down to the formation of adsorbed nitrogen species. Based on both experimental and theoretical studies, it is concluded that the ammonia decomposition is initiated by stripping of hydrogen from ammonia molecules via adsorbed oxygen atoms, whereas hydroxyl groups dominate in the further dehydrogenation of ammonia fragments.

3.2. Product distribution in ammonia oxidation under ambient pressure conditions

Distribution of reaction products vs. temperature is shown in Fig. 3 for the first heating and cooling cycles of a fresh Pt foil catalyst, with a feed containing an excess of O_2 over NH_3 (4.5 vol% O_2, 3 vol% NH_3). The catalytic reaction was measured at each temperature for 1 h. The only reaction products other than H_2O were N_2, N_2O, and NO. Nitrogen was the main product at low temperatures and was first observed at 423 K. At this temperature small amounts of N_2O are produced as well. An increase in temperature resulted in increasing formation of nitrogen and nitrous oxide. NO was detected at 623 K and became the dominating product at higher temperatures, and N_2 and N_2O formation passed through a maximum at 623 and 723 K, respectively.

Whereas steady-state catalyst operation is achieved at 423–623 K after an initial activation period, an ongoing time-dependent activation of the catalyst was observed at 723 and 823 K. This results in a different product distribution during cooling in the first temperature cycle (Fig. 3), with enhanced formation of nitrogen and nitrous oxide in the temperature range from 400 to 723 K. The activation of the catalyst is permanent: when the temperature program is repeated over the same Pt-foil catalyst, product formation during cooling in the first temperature cycle and during heating in the second cycle are almost the same. Further activation at

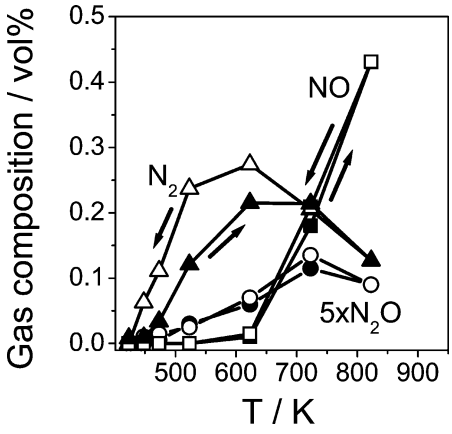

Fig. 3. Product distribution vs. temperature for temperature-programmed ammonia oxidation over Pt foil in micro-structured reactor (feed 250 ml/min, 3% NH_3, 4.5% O_2, balance Ar + Ne; filled symbols indicate the heating branch, open symbols indicate the cooling branch).

723 and 823 K is observed in the second temperature cycle, but the hysteresis is less pronounced. Increasing the time on stream at each temperature level to 24 h during heating and to ∼ 12 h during cooling results in a more significant hysteresis of product formation versus temperature. At 823 K no constant activity could be reached within 24 h, indicating an ongoing change on the catalyst surface.

The increase in catalyst activity in the first temperature cycle appears to be more significant at lower temperatures. This indicates either that Pt is activated only for low-temperature ammonia oxidation or the activation is masked by mass transfer limitations at higher temperatures. As mentioned above, the catalyst activity does not differ significantly between the cooling branch of the first temperature cycle and the heating branch of a second temperature cycle. Thus, we carried out the test for mass-transfer limitations by activating Pt foil in a first temperature cycle with Ar (3% NH_3, 4.5 vol% O_2, 250 ml/min) and comparing the results with a following second temperature cycle with He instead of Ar. The conversion curves start to deviate slightly at 473 K and significantly at 523 K. This indicates an influence of mass transfer on reaction rates starting at about 523 K on activated Pt foil or about 623 K over fresh Pt foil. Activation of Pt catalyst during repeated temperature cycles in ammonia oxidation would therefore be masked by mass-transfer limitations. Both the onset of a continuing activation and the test for mass-transfer limitation indicate a maximum temperature of roughly 523–623 K for steady-state tests of intrinsic kinetics.

To investigate the influence of feed composition on product formation in the ammonia oxidation, the reaction was also studied over a fresh Pt foil catalyst with an NH_3/O_2 ratio of 1. The product gas composition at different temperatures is shown in Fig. 4. Less NO and N_2O are produced compared with the previously discussed oxygen-rich feed. N_2 becomes the main product throughout the whole temperature range. NO production increases with temperature. Formation of N_2 and N_2O passes through a maximum around

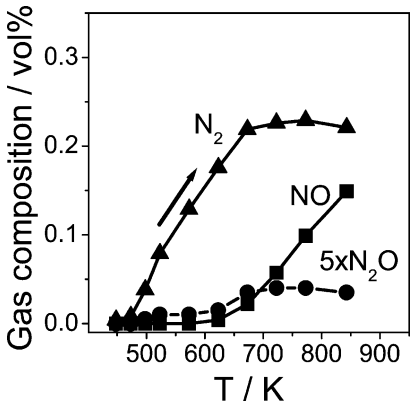

Fig. 4. Product distribution vs. temperature for temperature-programmed ammonia oxidation over Pt foil in microstructured reactor (feed 400 ml/min, 3% NH_3, 3% O_2, balance Ar + Ne; filled symbols indicate the heating branch).

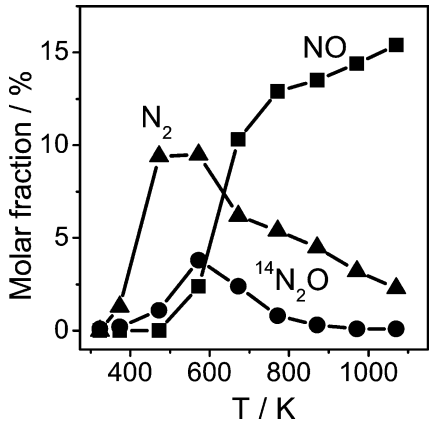

Fig. 5. Molar fractions of N_2O, NO and N_2 when a mixture of $NH_3/O_2/Ne = 1/1/1$ was pulsed in the TAP reactor over Pt gauze at different temperatures.

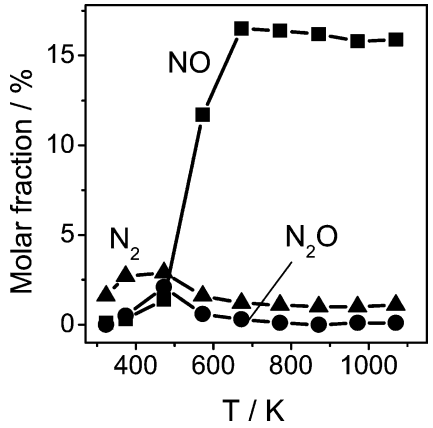

Fig. 6. Molar fractions of N_2O, NO and N_2 on pulsing a mixture $NH_3/O_2/Ne = 1/2/1$ in the TAP reactor over Pt gauze at different temperatures.

773 K. Both maxima are shifted toward higher temperatures as compared with those previous experiments using an excess of oxygen.

3.3. Product distribution in ammonia oxidation under transient vacuum conditions

In contrast to pulsing of NH_3 over Pt gauze without gas-phase oxygen (Fig. 2, Section 3.1), N_2, NO, and N_2O were formed when mixtures $NH_3/O_2/Ne = 1/1/1$ and $NH_3/O_2/Ne = 1{:}2{:}1$ were pulsed over Pt gauze ($p < 6$ Pa) (Figs. 5 and 6). H_2O was the only hydrogen-containing reaction product. The formation of N_2O in these experiments was proved by pulsing of a NH_3/O_2 mixture containing isotopically labeled ammonia ($^{15}NH_3$). No signal at AMU 44.0, which is related to CO_2 formation, was observed in these experiments at any temperature (Fig. 7). Short-lived intermediates such as NH_2, NH, and HNO were not detected in the gas phase when the respective AMUs were monitored. All of the products observed in the catalytic tests using Pt gauze are formed catalytically, since the transient experiments were carried out in the Knudsen diffusion regime, where interactions in the gas phase are unlikely.

Similar to results of ambient-pressure experiments (Section 3.2), the product distribution is a function of temperature (Figs. 5 and 6). Upon pulsing of a $NH_3/O_2/Ne = 1/1/1$ mixture, the formation of N_2O starts above 473 K (Fig. 5). After passing through a maximum at ca. 600 K, its amount decreases continuously with a further increase in temperature. N_2 was the only nitrogen-containing product at 373 K; its concentration passes through a maximum at ca. 600 K. NO appears in the gas phase above 500 K and becomes the main product at higher temperatures (Fig. 5). When the ratio of O_2–NH_3 is increased from 1 to 2, the selectivity for N_2O and NO (Fig. 6) increases. This is in good agreement with results obtained at ambient pressure (Section 3.2) and literature data on steady-state ambient pressure ammonia oxidation [48]. From Fig. 6 it is also clear that the maxima of N_2 and N_2O formation are shifted to a lower temperature (473 K) in the excess of oxygen. NO appears in the gas phase at lower temperature, and its content increases with rising temperature more strongly as compared with a mixture with $NH_3/O_2/Ne = 1/1/1$.

3.4. Product distribution in ammonia oxidation under UHV conditions

Results of temperature-programmed ammonia oxidation over cleaned Pt(533) are shown in Fig. 8 for two different ratios of NH_3/O_2 (1/1 and 1/3). Reaction starts around 500 K with the formation of N_2, which is the only nitrogen-containing product at low temperatures (< 600 K). NO was observed above 600 K. The formation of NO increases with temperature and decreases slightly above 900 K. AMU 44, which belongs to N_2O and background CO_2, was monitored throughout the experiment. Since no change in the intensity of the signal at AMU 44 was observed, no formation of N_2O was identified in detectable amounts. A slightly higher catalyst activity was observed in the cooling branch (not shown

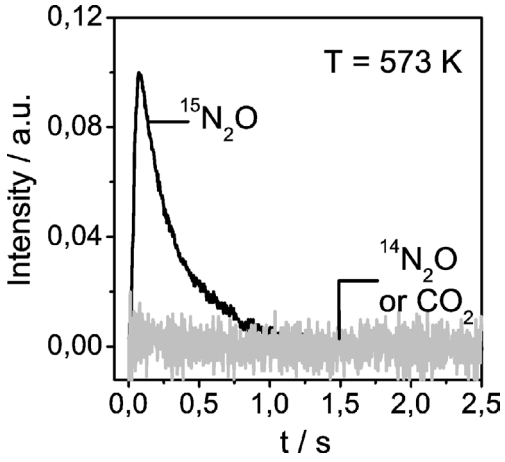

Fig. 7. Transient responses recorded during pulsing a mixture of $^{15}NH_3/O_2/Ne = 1/1/1$ in the TAP reactor over Pt gauze at 573 K.

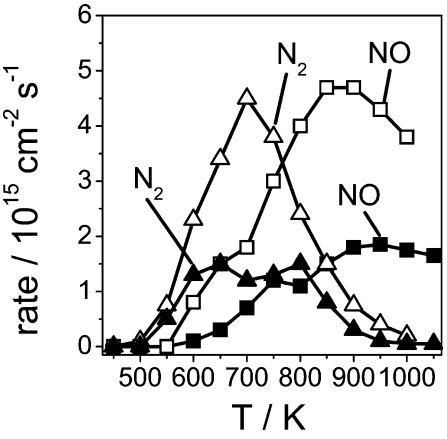

Fig. 8. Temperature dependence of the N_2 and NO production on Pt(533) under UHV conditions using reaction mixtures with NH_3/O_2 ratios of 1 (closed symbols) and 0.3 (open symbols) at fixed $p_{NH3} = 1 \times 10^{-2}$ Pa.

here), as previously reported and discussed for large oxygen excess [11]. It was also shown before in detail [11] that the break in reaction rates around 700 K (Fig. 8) can be explained by a reversible change in catalyst morphology. LEED and STM indicated the formation of double-atomic steps, which disappeared with further heating [49].

Product formation over Pt(533) strongly depends on the ratio of NH_3 to O_2 (Fig. 8). A higher partial pressure of oxygen results in increased N_2 formation at all temperatures, but this effect is more pronounced at low temperatures. The onset of nitrogen production shifts slightly toward lower temperatures. A higher oxygen/ammonia ratio also improves NO formation in the whole temperature range where nitric oxide is formed. Selectivity for NO is increased (Fig. 8).

3.5. Reaction-induced changes of surface morphology

SEM images of fresh Pt-foil and Pt-gauze catalysts are given in Figs. 9a, b and Fig. 10a, respectively. Some textural damage caused by the manufacturing process is seen. In general, the Pt surface is smooth and flat with occasional holes.

Surface morphology of the Pt-foil catalyst changes dramatically after its use in ammonia oxidation under ambient pressure conditions during 12 h of the temperature ramp from 293 to 823 K and back to 293 K. The surface is visibly roughened (Figs. 9c, d), which is accompanied by an increase in catalyst activity. Small crystals start to grow from the surface in some domains (Fig. 9d), and other areas are covered by flat triangular structures growing on top of each other. All new surface structures exhibit sharp edges. The crystal planes appear to be flat and some of the planes contain holes. The further development of these structures was observed when the Pt foil was used under reaction conditions for a longer period of time (10 days). The respective SEM images are shown in Fig. 9e and f. Crystal structures on the surface became larger. Crystals seem to be arranged in layers on top of each other. They do not appear to protrude so much from the surface, but rather preferably arrange parallel to the surface and parallel to each other. Structures no longer feature sharp edges, but look rather smooth and rounded. The occasional appearance of rounded holes in crystal surfaces might indicate local melting. As observed, the changes in Pt morphology under reaction conditions led to roughening of the platinum surface. Because of the small sample size the respective surface areas could not be measured with any satisfactory accuracy. Hence, a proportionality could not be established between the increase in catalyst activity and the increase in surface area, and no statement can be made about whether the activation is due to the formation of differently active sites.

In contrast to ambient-pressure ammonia oxidation, no surface restructuring is visible in SEM after repeated exposure of Pt gauze catalyst to oxygen pretreatment at 1073 K and ammonia oxidation under transient conditions (323–1073 K). Similar results were obtained for a single crystal Pt(533), which was used for ammonia oxidation under UHV conditions. LEED and STM demonstrated that the microscopic structure of Pt(533) changes reversibly under reaction conditions [11]. Under certain conditions a doubling of the step height of the initially monoatomic steps on Pt(533) occurs that is associated with a change in selectivity from preferential N_2 formation to NO as the main product. Under the relatively mild reaction conditions of an UHV experiment, however, the microscopic structural changes are not associated with variations in the macroscopic surface topography (Fig. 11a). Only by tilting the crystal can some kind of structure be made visible (Fig. 11b), which is ascribed to the initial procedure for polishing the crystal. Faceting and growth of smaller crystals from the surface are not observed by SEM.

4. Discussion

Section 4.1 gives a possible explanation for morphological changes induced on the surface of different Pt materials during ammonia oxidation over a broad range of total pres-

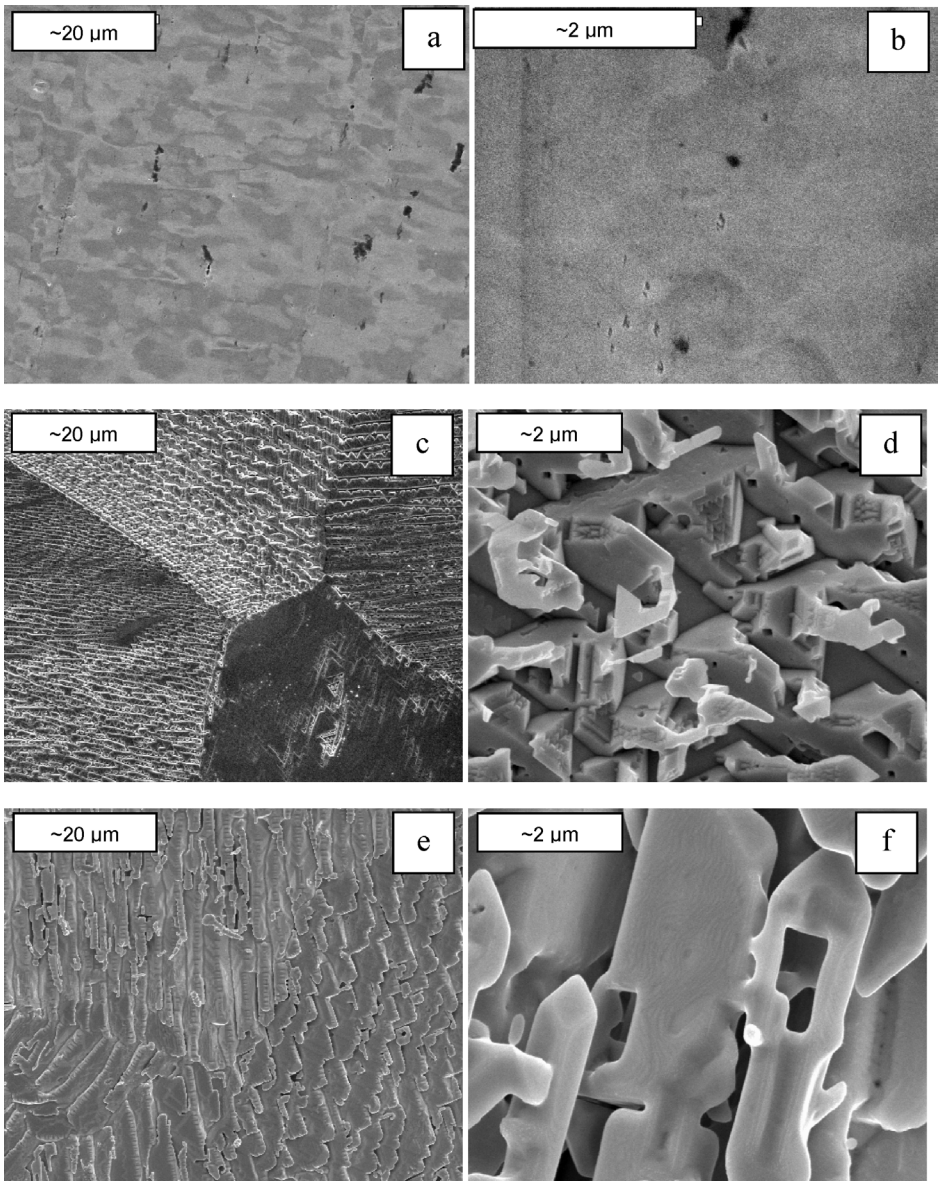

Fig. 9. SEM of Pt foil before and after use in ammonia oxidation in micro-structured reactor: fresh Pt foil (a, b), Pt foil after temperature programmed ammonia oxidation at 293–823 K for 12 h (c, d) and Pt foil after temperature programmed ammonia oxidation at 293–823 K for 10 d (e, f).

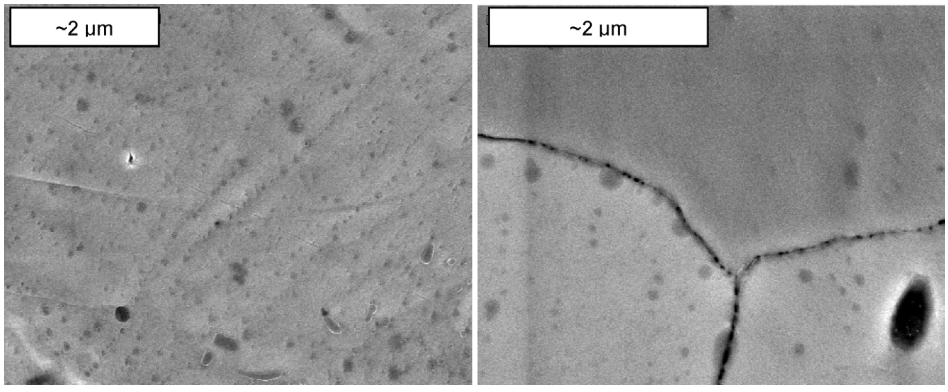

Fig. 10. SEM of Pt gauze before (left) and after (right) the studies of ammonia oxidation under transient conditions in the TAP reactor.

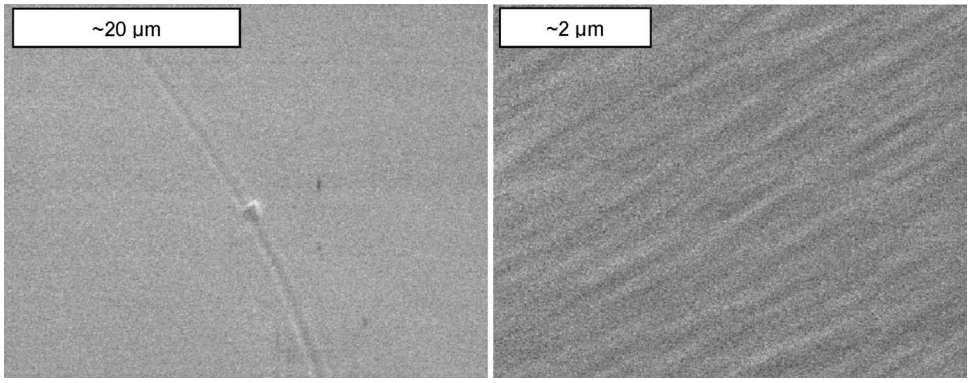

Fig. 11. SEM of Pt(533) after repeated ammonia oxidation under UHV conditions.

sures (10^{-3}–10^{5} Pa). A relationship between these changes and catalytic properties is suggested. The influence of total pressure and Pt material on product distribution in the ammonia oxidation reaction is discussed in Section 4.2.

4.1. Influence of reaction conditions on the surface morphology of different Pt materials

No macroscopic roughening or restructuring of the Pt surface was observed by SEM up to a 5000-fold magnification, when Pt gauze or a Pt(533) single crystal was repeatedly exposed to ammonia oxidation under vacuum in the TAP reactor and UHV conditions, respectively. This is in agreement with previous data in the literature. Using optical microscopy, Gland and Korchak [20] did not see faceting of Pt single crystals used in UHV ammonia oxidation. Pignet and Schmidt [13] studied restructuring phenomena of Pt wires that had been used for many hours in ammonia oxidation at a total pressure of 10 Pa. They concluded that the surface stays "quite smooth."

In contrast to low-pressure ammonia oxidation, under industrial ammonia oxidation conditions, growth of so-called cauliflowers significantly changes the surface of Pt wire. Although this final cauliflower state of catalyst etching was not found in the present work, results from Figs. 9e and f seem to be similar to initial stages of such cauliflower growth. The phenomenon has been systematically studied by SEM on Pt wires [15–17] and spheres ($d \sim 0.6$ mm) [50] that were prepared under flow conditions of ammonia oxidation with a total pressure of 1 bar and various feed compositions. Exposure times were in the range of 15 min [15] to 386 h [17]. All of the investigations of catalytic etching have been carried out in the regime of ignited ammonia oxidation (above 900 K). The results of our experiments make it possible for the first time to examine surface morphology after reaction at 650–850 K with reactant partial pressures in the kPa range. McCabe and co-workers [16] obtained a "phase diagram" illustrating the effect of temperature (973–1773 K) and NH_3/O_2 ratio on surface morphology. Depending on the gas-phase composition and temperature, different types of facets were observed. Surface restructuring was more extensive and rapid in an ammonia/air mixture as compared with pure oxygen or ammonia. Lyubovski and Barelko [15] observed in a time-resolved SEM study that restructuring of Pt wire used for ammonia oxidation at ca. 1373 K can be divided into two phases. They defined an initial phase of formation of parallel facets. The facets are about 5 µm apart. These facets somehow resemble the pattern shown in Fig. 9c. Another similarity between the present results and their work is the fact that not all grains are etched to the same extent, perhaps because of different initial crystal orientations. The initial phase of reaction-induced restructuring of the surface [15] is followed by formation of individual and randomly located microcrystals with well-formed crystal faces, where the new crystals extend into the surrounding volume. This state of progressed etching describes a high-resolution image as shown in Fig. 9d quite well. Finally, those authors observed a slow growth of larger crystals ($\sim$ 30 µm long, 5 µm thick) that seems to be the beginning of cauliflower growth. No such features were observed in the present study. According to Nilsen et al. [17], these cauliflowers are associated with ammonia oxidation for a long time and at temperatures above 1073 K. Ammonia oxidation at lower temperatures produces what they call "nodules;" this might resemble an enlarged version of the structures developed in the microstructured reactor foil after extended periods of ammonia oxidation (Figs. 9e, f).

Taking into account the above discussion, the differences in surface restructuring that occur after the ammonia oxidation reaction under low and ambient pressure conditions can be explained as follows. Since significant surface restructuring of Pt requires the presence of NH_3 and O_2 at the same time [16], the reaction intermediates are suggested to be responsible for the structural changes. This assumption is supported by results of Nilsen et al. [17], who found no significant etching of Pt surfaces when passing NO, N_2O, or H_2O over the catalyst. The concentration of reaction intermediates on the surface may play a key role in the restructuring process. A similar idea was previously put forward by McCabe and co-workers [16]. These authors concluded that Pt restructuring depends on the total amount of NH_3 and O_2 passed over the catalyst. Thus it can be suggested that the failure to observe any macroscopic changes in surface morphology by SEM after ammonia oxidation at low reac-

tant pressures is due to considerably lower amounts of NH_3 and O_2 to which Pt(533) single crystal or Pt gauze were exposed under UHV and vacuum conditions. For comparison, ca. 5×10^{-7} mol/cm^2 of ammonia was pulsed over Pt gauze during ammonia oxidation in the TAP reactor, Pt(533) was exposed to about 10^{-4} mol/cm^2 of ammonia during temperature ramping, and ca. 10 mol/cm^2 of NH_3 was passed over the Pt foil during ammonia oxidation (3 vol% NH_3 and O_2, respectively) in the microstructured reactor at ambient pressure for 10 h.

The above changes in catalyst morphology must also be reflected on an atomic scale. Previous experiments with single crystals of Pt(533) and Pt(443) did demonstrate that the step structure changes easily, even under mild reaction conditions, and, furthermore, that the activation barrier for this microscopic restructuring is much lower under reaction conditions than in the presence of one reactant only [49]. Detailed, atomically resolving STM studies have revealed that the mobility of surface Pt atoms is dramatically increased in the presence of adsorbates such as atomic hydrogen [51]. Quantum chemical calculations of ammonia adsorption on stepped Pt(111) surfaces indicate a similar trend that can be attributed mechanistically to a lowering of the binding strength of a Pt atom bound to the substrate if it is attached to an adparticle [52]. Nevertheless, under vacuum conditions the buildup of such changes on an atomic level was not sufficient for detection by SEM.

Qualitatively the observations made with the single-crystal planes are in agreement with the results obtained with polycrystalline Pt under much higher pressure. An additional factor, which has to be taken into account, is the penetration of oxygen into the Pt bulk under reaction conditions, which was established recently [53]. This phenomenon is probably connected with restructuring of the surface, whereby the surface will open up channels for oxygen penetrating into the Pt bulk. The extent to which the formation of new oxygen species just accompanies the restructuring of the surface or whether it is the actual driving force for restructuring need to be shown in future investigations. Mechanistically, a bridge needs to be established between the microscopic structural changes observed with LEED and STM and the macroscopic topographical changes that are seen with SEM on Pt catalysts exposed to high-pressure reaction conditions.

4.2. Effect of total pressure on catalytic performance of different Pt materials

Independently of the total pressure, at temperatures below 700 K nitrogen is the main product of ammonia oxidation over Pt(533) single crystal, knitted Pt (gauze), and Pt foil. The temperature dependence of N_2 formation passes through a maximum. The position of the maximum for N_2 production is a function of the ratio of NH_3 to O_2. The higher the ratio, the higher is the temperature of the maximum (Figs. 3–6). In an extreme case, such as ammonia pulsing without gas-phase oxygen, N_2 formation increases continuously with increasing temperature (Fig. 2). A similar tendency was previously reported for ammonia oxidation over Pt(100) with molecular beams at about 10^{-8} Pa [22] and over stepped Pt 12(111) × (111) [20]. The shift of the maximum in N_2 formation toward lower temperature with increasing oxygen partial pressure may be explained by the fact that an increase in oxygen partial pressure results in a higher surface coverage by oxygen species, which favors oxidation of surface nitrogen species to NO over their recombination to N_2. Therefore N_2 formation decreases at higher temperatures, when NO is formed. On the other hand, the theoretical and experimental results show that adsorbed O and OH species contribute to the hydrogen stripping from NH_3 molecules (Section 3.1), whereby ammonia conversion at low temperatures is increased, and thus to N_2 formation. In addition, from our previous work on high-temperature (1023–1073 K) ammonia oxidation, it was concluded that the oxygen coverage and the nature of oxygen species are important in NO formation [26].

For all types of Pt catalyst, NO formation during NH_3 oxidation in the presence of gas-phase O_2 starts at ca. 550 K and dominates above 600–700 K. These findings are consistent with UHV studies reported in the literature. Gland and Korchak [20] studied the ammonia oxidation over stepped Pt 12(111) × (111) in the pressure range from 10^{-8}–10^{-6} Pa, which is an order of magnitude below the pressure in the present UHV experiments. Nitrogen was the main product at low temperatures. Significant formation of NO started at about 570 K; NO was the main product at high temperatures. However, its production decreased at the highest temperatures under vacuum conditions. The decline in NO formation above 900 K is due to a decrease in the sticking coefficients of the reactants with increasing temperature. It has to be emphasized that N_2O was not observed in any of the above-described UHV studies or in the present study over a Pt(533) single crystal under UHV conditions. In contrast to these UHV results, N_2O was observed in the present study when a mixture of ammonia and oxygen was pulsed over knitted Pt gauze at about 6 Pa in the TAP reactor at temperatures from 400 to 800 K. The formation of N_2O was already demonstrated at temperatures above 1073 K under transient conditions [26]. However, the cited study was performed at a peak pressure of 160 Pa, which is significantly higher than in the present study. In contrast to the lower pressures (Knudsen diffusion regime), at which all homogeneous reaction steps are suppressed, at higher pressures, that is, in the regime of molecular diffusion, N_2O formation might be also influenced by gas-phase interactions. The proof of N_2O in the Knudsen diffusion regime (ca. 6 Pa) seems therefore noteworthy, since this product was not observed at similar pressures of ca. 10 Pa in earlier studies [12,13]. Aside from this, the distribution of N_2 and NO formation versus temperature is similar, and raising the oxygen content has the same effects of increasing NO selectivity and shifting the maxima of NO and N_2 formation toward lower temperatures. N_2O was also observed, when ammonia oxidation was per-

formed over Pt foil in the microstructured reactor at ambient pressure (Section 3.2). N_2O formation peaks around 750 K (Figs. 3 and 4). It should be mentioned in particular that under ambient pressure catalytic tests were carried out under conditions eliminating ignition. This confirms the advantage of microstructured reactors for the study of highly exothermic ammonia oxidation, as was established before by Rebrov et al. [24] at lower temperatures (< 650 K). A study by Pignet and Schmidt [12] exemplifies the difficulties usually associated with studies of ammonia oxidation close to ambient pressure. They investigated the reaction over Pt wires and were unable to obtain any temperature-controlled catalytic data with a feed of 7.5% NH_3 and 20% O_2 in Ar due to ignition of the reaction feed.

The present study on ammonia oxidation within a broad total-pressure range and under isothermal conditions reveals that different Pt materials, single Pt(533) crystal, knitted Pt gauze, and a Pt foil, show very similar catalytic performance with respect to NO and N_2 formation. The main difference between ammonia oxidation over Pt(533) single crystal under UHV conditions and in tests over polycrystalline materials at higher pressures (> 1 Pa) is the absence of N_2O under UHV. With the present knowledge, we cannot exclude the possibility that N_2O is preferentially formed over polycrystalline materials only. However, we assume that the total pressure plays the most important role, as discussed below.

The temperature of maximum N_2O formation under vacuum conditions in the TAP reactor is lower by about 180 K than that under ambient pressure conditions for a similar ratio of NH_3/O_2 (Figs. 3–6). N_2O formation is shifted toward lower temperatures with decreasing absolute pressure. If this trend is linearly extrapolated to lower pressures (UHV conditions), the maximum of N_2O selectivity would be in a temperature range where hardly any ammonia is converted. Since N_2O formation is only heterogeneously catalyzed (Section 3.3), surface coverage by intermediates, from which N_2O is formed, obviously plays an important role. Three different mechanistic models for N_2O formation are discussed in the literature:

- N_2O is formed via recombination of two assumed HNO intermediates [Eq. (1)] [54,55];
- N_2O originates from recombination of two surface NO molecules [Eq. (2)] [56];
- N_2O is formed via interaction between NH_x and NO [Eq. (3)] [27].

$$\mathrm{HNO\text{–}s + HNO\text{–}s \rightarrow N_2O + H_2O + 2s;} \quad (1)$$

$$\mathrm{NO\text{–}s + NO\text{–}s \rightarrow N_2O + O\text{–}s + s;} \quad (2)$$

$$\mathrm{NO\text{–}s + NH_x\text{–}s + O\text{–}s \rightarrow N_2O + H_xO + 3s.} \quad (3)$$

It should be emphasized that the above equations do not represent elementary reaction steps, but are typically lumps of elementary step. All proposed reaction mechanisms of N_2O formation [Eqs. (1)–(3)] include the interaction of two adsorbed species on the surface. So without stating which mechanism of N_2O formation is valid, a possible explanation for the effect of total pressure on N_2O formation might be the requirement of high surface coverage of reactants or intermediates [Eqs. (1)–(3)] to form nitrous oxide. Usually, a high surface coverage is promoted by lower temperature and high pressure, and only under such conditions was a significant N_2O selectivity observed experimentally. It was shown that for ambient pressure conditions (Section 3.2), N_2O formation undergoes a maximum at 750 K. For lower pressures of the TAP reactor, the highest N_2O concentration was observed at 573 K, that is, ca. 180 K lower than at ambient pressure. For reduced pressure, the temperature range where a significant coverage of the surface with adsorbates is expected also shifts to lower temperatures. The maximum of N_2O formation (with N_2O originating from a surface reaction of second order) should also shift to a lower temperature. This was indeed observed experimentally in TAP experiments. At even lower pressures of UHV the surface coverage is probably too low to form N_2O in amounts that can be analytically detected. Thus, a possible explanation for the pressure-related differences in N_2O production is the described kinetic effect, although mechanistic effects or the influence of surface defects on nitrous oxide production cannot be excluded.

5. Conclusions

Different total pressures (10^{-3}–10^5 Pa) and catalytic materials (Pt single crystal, knitted Pt gauze, and Pt foil) were applied in the oxidation of ammonia. These variables did not influence the general temperature dependence of N_2 and NO formation. That is to say, the “pressure gap” can be bridged for the catalysis of the main reaction paths. N_2 is preferentially formed at low temperatures and passes through a maximum. NO formation increases continuously with temperature and decreases slightly only at the highest temperatures applied and at low pressure, because of a decrease in the sticking coefficients of reactants.

The main difference between UHV (10^{-3} Pa) and TAP (6 Pa) and ambient pressure conditions (100 kPa) is the absence of the reaction product N_2O under UHV conditions when a stepped Pt(533) single crystal is used. This can be explained by the fact that N_2O formation strongly depends on surface coverage by reaction intermediates, which is a function of partial pressures of feed and product molecules.

No significant restructuring of the surfaces of the different Pt materials was observed by SEM when Pt gauze and Pt(533) single crystal were repeatedly used for ammonia oxidation under vacuum in the TAP reactor and UHV conditions, respectively. In contrast to low-pressure ammonia oxidation, significant reconstruction of the Pt surface occurs after ammonia oxidation at ambient pressure. The pressure dependence of surface-morphology changes is related to the extent of catalyst exposure to reactants. The surface roughening is accompanied by an increase in activity of the foil

catalyst. This effect will be studied more closely in future work.

Acknowledgments

The authors thank Deutsche Forschungsgemeinschaft (DFG) for financial support in the frame of the competence network SPP1091, “Bridging the gap between real and ideal systems in heterogeneous catalysis.” V. Kondratenko thanks the Institute for Applied Chemistry Berlin-Adlershof e.V. for a Ph.D. fellowship. The provision of SEM results by Gisela Weinberg and Robert Schlögl was highly appreciated.

References

[1] M. Bodenstein, Z. Elektrochem. 41 (1935) 466.
[2] L. Apelbaum, M. Temkin, Z. Phiz. Khim. 22 (1948) 179.
[3] L. Andrussow, Z. Angew. Chem. 63 (1951) 350.
[4] Y.M. Fogel, B.T. Nadytko, V.F. Rybalko, V.I. Shvachko, I.E. Korobchanskaya, Kin. Katal. 5 (1964) 496.
[5] V.I. Atroshchenko, S.I. Kargin, in: Nitric Acid Technology, Khimia, Moscow, 1970, p. 496.
[6] V.I. Atroshchenko, in: Kinetics of Heterogeneous Catalytic Reactions under Pressure, Nauka, Moscow, 1974, p. 169.
[7] M. Kim, S.J. Pratt, D.A. King, J. Am. Chem. Soc. 122 (2000) 2409.
[8] J.M. Bradley, A. Hopkinson, D.A. King, J. Phys. Chem. 99 (1995) 17032.
[9] J.L. Gland, V.N. Korchak, J. Catal. 53 (1978) 9.
[10] M. Asscher, W.L. Guthrie, T.-H. Lin, G.A. Somorjai, J. Phys. Chem. 88 (1984) 3233.
[11] A. Scheibe, S. Gunther, R. Imbihl, Catal. Lett. 86 (2003) 33.
[12] T. Pignet, L.D. Schmidt, Chem. Eng. Sci. 29 (1974) 1123.
[13] T. Pignet, L.D. Schmidt, J. Catal. 40 (1975) 212.
[14] E.V. Rebrov, M.H.J.M. de Croon, J.C. Schouten, Chem. Eng. J. 90 (2002) 61.
[15] M.R. Lyubovsky, V.V. Barelko, J. Catal. 149 (1994) 23.
[16] R.W. McCabe, T. Pignet, L.D. Schmidt, J. Catal. 32 (1974) 114.
[17] O. Nilsen, A. Kjekshus, H. Fjellvag, Appl. Catal. A 207 (2001) 43.
[18] A.C.M. van den Broek, J. van Grondelle, R.A. van Santen, J. Catal. 185 (1999) 297.
[19] J.J. Ostermaier, J.R. Katzer, W.H. Manogue, J. Catal. 33 (1974) 457.
[20] J.L. Gland, V.N. Korchak, J. Catal. 53 (1978) 9.
[21] W.D. Mieher, W. Ho, Surf. Sci. 322 (1995) 151.
[22] J.M. Bradley, A. Hopkinson, D.A. King, J. Phys. Chem. 99 (1995) 17032.
[23] J. Pérez-Ramírez, F. Kapteijn, K. Schöffel, J.A. Moulijn, Appl. Catal. B 44 (2003) 117.
[24] E.V. Rebrov, M.H.J.M. de Croon, J.C. Schouten, Catal. Today 69 (2001) 183.
[25] E.V. Rebrov, S.A. Duinkerke, M.H.J.M. de Croon, J.C. Schouten, Chem. Eng. J. 93 (2003) 201.
[26] J. Pérez-Ramírez, E.V. Kondratenko, V.A. Kondratenko, M. Baerns, J. Catal. 227 (2004) 90.
[27] J. Pérez-Ramírez, E.V. Kondratenko, Chem. Commun. (2004) 376.
[28] R.J. Farrauto, C.H. Bartholomew, in: Fundamentals of Industrial Catalytic Processes, Chapman & Hall, London, 1997, p. 481.
[29] E. Bergene, PhD thesis, Surface characterisation of Pt and Pt/Rh gauze catalysts, Trondheim, 1990, p. 119.
[30] E. Bergene, O. Tronstadt, A. Holmen, J. Catal. 160 (1996) 141.
[31] J.T. Gleaves, J.R. Ebner, T.C. Kuechler, Catal. Rev.-Sci. Eng. 30 (1) (1988) 49.
[32] J.T. Gleaves, G.S. Yablonsky, P. Phanawadee, Y. Schuurman, Appl. Catal. A 160 (1997) 55.
[33] S. Walter, PhD thesis, Mikrostrukturreaktoren für selektive Oxidationsreaktionen–Isopren zu Citraconsäureanhydrid, Erlangen, 2003, p. 303.
[34] G. Kresse, J. Furthmüller, J. Comput. Mat. Sci. 6 (1996) 15.
[35] G. Kresse, J. Furthmüller, J. Phys. Rev. B 54 (1996) 11169.
[36] D. Vanderbilt, Phys. Rev. B 41 (1990) 7892.
[37] G. Kresse, J. Hafner, J. Phys.: Condens. Matt. (1994) 8245.
[38] J.P. Perdew, in: P. Ziesche, H. Eschrig (Eds.), Electronic Structure of Solids’91, Akademie, Berlin, 1991, p. 11.
[39] A. Bogicevic, K.C. Hass, Surf. Sci. 506 (2002) L237.
[40] B. Hammer, Surf. Sci. 459 (2000) 323.
[41] B. Hammer, Faraday Discuss. 110 (1998) 323.
[42] H. Jónsson, G. Mills, K.W. Jacobsen, in: B.J. Berne, G. Ciccotti, D.F. Coker (Eds.), Classical and Quantum Dynamics in Condensed Phase Simulations, World Scientific, Singapore, 1998, p. 385.
[43] G. Henkelman, G. Jóhannesson, H. Jónsson, in: Theoretical Methods in Condensed Phase Chemistry, Progress in Theoretical Chemistry and Physics, vol. 5, Kluwer-Academic Publishers, Dordrecht, The Netherlands, 2000, p. 269.
[44] G. Henkelman, H. Jónsson, J. Chem. Phys. 113 (2000) 9978.
[45] G. Henkelman, B.P. Uberuaga, H. Jónsson, J. Chem. Phys. 113 (2000) 9901.
[46] D.P. Sobczyk, A.M. de Jong, E.J.M. Hensen, R.A. van Santen, J. Catal. 219 (2003) 156.
[47] W.K. Offermans, A.P.J. Jansen, G.J. Kramer, R.A. van Santen, EuropaCat-VI, Innsbruck, 2003.
[48] R.M. Heck, J.C. Bonacci, W.R. Hatfield, T.H. Hsiung, Ind. Eng. Chem. Process Des. Dev. 21 (1982) 73.
[49] A. Scheibe, PhD thesis, Gestufte Platineinkristalloberflaechen als Modellsystem fuer die katalytische Ammoniakoxidation mit Sauerstoff, Hannover, 2003, p. 177.
[50] M. Flytzani-Stephanopoulos, S. Wong, L.D. Schmidt, J. Catal. 49 (1977) 51.
[51] T.R. Linderoth, S. Horch, L. Petersen, S. Helveg, E. Laegsgaard, I. Stensgaard, F. Besenbacher, Phys. Rev. Lett. 82 (1999) 1494.
[52] W.K. Offermans, in preparation.
[53] S. Günther, R. Krähnert, in preparation.
[54] L. Andrussow, Z. Angew. Chem. 39 (1926) 321.
[55] K. Otto, M. Shelef, J.T. Kummer, J. Phys. Chem. 74 (1970) 2690.
[56] P. Denton, Y. Schuurman, A. Giroir-Fendler, H. Praliaud, M. Primet, C. Mirodatos, C.R. Acad. Sci., Ser. IIc: Chim. 3 (2000) 437.